Journal of Peptide Science
J. Pept. Sci. 2006; **12**: 748–757
Published online in Wiley InterScience (www.interscience.wiley.com). DOI: 10.1002/psc.808

JOURNAL OF PEPTIDE SCIENCE

Synthesis, conformation, and bioactivity of novel analogues of the antiviral lipopeptide halovir A

ANDREA DALLA BONA,[a] FERNANDO FORMAGGIO,[a] CRISTINA PEGGION,[a] BERNARD KAPTEIN,[b] QUIRINUS B. BROXTERMAN,[b] STEFANIA GALDIERO,[c,d,e] MASSIMILIANO GALDIERO,[d,f] MARIATERESA VITIELLO,[f] ETTORE BENEDETTI,[c,d,e] and CLAUDIO TONIOLO[a]*

[a] Department of Chemistry, University of Padova, 35131 Padova, Italy
[b] DSM Research, Life Sciences, Advanced Synthesis and Catalysis, 6160 MD Geleen, The Netherlands
[c] Department of Biological Sciences, Division of Biostructures, University of Naples 'Federico II', 80134 Napoli, Italy
[d] Centro Interuniversitario di Ricerca sui Peptidi Bioattivi, University of Naples 'Federico II', 80134 Napoli, Italy
[e] Istituto di Biostrutture e Bioimmagini, CNR, 80134 Napoli, Italy
[f] Department of Experimental Medicine, 2nd University of Naples, 80138 Napoli, Italy

Received 17 July 2006; *Revised 20 September 2006*; *Accepted 20 September 2006*

Abstract: We synthesized by solution-phase methods three analogues, [L-Leu^6-OMe], [L-(αMe)Leu^3, L-Leu^6-OMe], and [L-(αMe)Val^4, L-Leu^6-OMe] of halovir A. The [L-Leu^6-OMe] analogue is known to be biologically equipotent to its naturally occurring, antiviral, lipopentapeptide amide parent compound. The preferred conformations of the L-(αMe)Leu- and L-(αMe)Val-containing analogues, with a potentially reinforced helicity, were compared with those of [L-Leu^6-OMe] halovir A and the natural peptide itself by use of a combination of FT-IR absorption and NMR techniques. Measurements of the antiviral activities against herpes simplex virus type-1 (HSV-1) of halovir A and its three analogues were also carried out. Interestingly, the [L-(αMe)Val^4, L-Leu^6-OMe] analogue exhibits the most significant activity in reducing HSV-1 infectivity, notably higher than that of halovir A itself. Copyright © 2006 European Peptide Society and John Wiley & Sons, Ltd.

Keywords: antiviral activity; C^{α}-methylated α-amino acids; peptide conformation; peptide synthesis; spectroscopy

INTRODUCTION

The peptaibols [1,2] are members of a family of short bioactive peptides, ranging in length from 5 to 19 amino acid residues, which have been isolated from a wide range of fungal sources. Most of them are capable of acting as antibiotics against specific bacteria and parasites. In general, their bioactivities are derived from their membrane-modifying properties [3–5]. More than 300 sequences of naturally occurring peptaibols have been identified so far, with the number increasing significantly on a yearly basis [6]. One of the prevailing characteristics of this family is the presence of noncoded α-amino acids, including the strongly helicogenic Aib residue [7,8].

Recently, Rowley *et al.* [9] reported the isolation, amino acid sequence, solution conformation, and bioactivity of a series of uncharged lipopeptaibols, termed *halovirs* A–E, extracted from a marine fungus of the genus *Scytalidium*. Interestingly, these compounds exhibit a rather unusual property for peptaibols, namely, they are potent *in vitro* inhibitors against HSV types 1 and 2. Infections with HSV-1 and -2 are ubiquitous, although there is a marked regional variation in prevalence throughout the world. Among various populations, between 60 and 95% are infected with HSV-1, and between 6 and 50% with HSV-2. Most initial and recurrent infections are asymptomatic or unrecognized. The clinical manifestations of HSV-1 and HSV-2 infections are diverse and represent a huge worldwide disease and economic burden. Most recurrent *Herpes labialis* can be regarded as only a nuisance; however, the complications of herpetic eye disease, encephalitis and the spread of skin infections are serious issues. Genital herpes, caused by both HSV-1 and HSV-2, and the feared complications of neonatal herpes are major targets for control [10]. No vaccines, despite repeated attempts, are yet available for prevention, but classical antivirals, such as nucleoside analogues, are the chemotherapies of choice. Nevertheless, HSV-resistant strains and the failure to completely relieve symptoms (especially in immunocompromised individuals) make it imperative that antivirals that utilize new mechanisms of action be developed.

Abbreviations: AcOH, acetic acid; (αMe)Leu, C^{α}-methyl leucine; (αMe)Val, C^{α}-methyl valine; DMEM, Dulbecco's modified Eagle's medium; EDC, *N*-ethyl,*N*′-[3-(dimethylamino)propyl] carbodiimide; EtOH, ethanol; HSV, herpex simplex virus; LDH, lactate dehydrogenase; Lol, leucinol; Myr, myristoyl; OMe, methoxy; PC, phosphatidylcholine; Z, benzyloxycarbonyl.

*Correspondence to: C. Toniolo, Department of Chemistry, University of Padova, via Marzolo 1, 35131 Padova, Italy;
e-mail: claudio.toniolo@unipd.it

The amino acid sequence of halovir A, the most active component of this family of terminally blocked pentapeptide amides, is as follows:

Myr-Aib[1]-L-Hyp-L-Leu-L-Val-L-Gln[5]-L-Lol (the configuration at C-4 of Hyp is *R*)

Salient features of the halovir sequences include a fatty acyl moiety (typically, myristic acid, C_{14}) linked to the terminal amino function and an Aib residue at position 1. The results of a qualitative NMR analysis of the secondary structure of halovir A in $CDCl_3$ and deuterated MeOH and DMSO solutions are consistent with the peptide chain adopting a 3_{10}-helical [11] structure. Looking at the 3D model of the peptide portion of halovir A in a 3_{10}-helix, the authors predicted an amphiphilic conformation with the polar Hyp[2] and Gln[5] side chains positioned on one face of the helix and the apolar Leu[3] and Lol side chains arranged on another face.

In a subsequent paper [12] Rowley *et al.* investigated the chemical structure–activity relationships of halovir A by synthesizing via solution methods a large set of peptide analogues with the aim of defining the key elements for an optimal viral inhibition. Their results demonstrated that an N^{α}-fatty acyl chain of at least 14 carbon atoms and an Aib-Hyp dipeptide sequence at the *N*-terminus are critical for a high antiviral activity. Interestingly, the [L-Leu[6]-OMe] analogue, the synthetic precursor of halovir A, showed a nearly equivalent anti-HSV-1 activity, but a slightly lower cytotoxicity.

Stimulated by the peculiar and attractive antiviral properties of halovir A and its remarkably small main-chain length, a great advantage in view of possible biomedical applications, we decided to synthesize additional analogues focusing on the enhancement of the amount of 3_{10}-helical structure without modifying the overall amphiphilic character of the peptide. As discussed by Rowley *et al.* [9], it is quite evident that the remarkable helicity of this peptide as short as an N^{α}-acylated pentapeptide amide should be related to the presence of the single Aib residue [7,8] in its sequence. We reasoned that replacing either L-Leu[3] or L-Val[4] with their C^{α}-methylated counterparts would have reinforced the halovir A helicity. Indeed, L-(αMe)Leu and L-(αMe)Val are two members of the class of C^{α}-methylated α-amino acids, the prototype of which is Aib, known to tightly fold the peptide main chain by virtue of the Thorpe–Ingold effect (C^{α}-tetrasubstitution) [8,13]. Therefore, to this end, we prepared by solution methods halovir A and its biologically equipotent [L-Leu[6]-OMe] analogue, already synthesized by Rowley *et al.* [12], and extended the synthetic effort to the [L-(αMe)Leu[3], L-Leu[6]-OMe] and [L-(αMe)Val[4], L-Leu[6]-OMe] analogues. Comparative conformational analyses in solution and antiviral assays were also performed on all four peptides.

MATERIALS AND METHODS

Synthesis and Characterization of Peptides

Melting points were determined using a Leitz (Wetzlar, Germany) model Laborlux 12 apparatus and were not corrected. Optical rotations were measured using a Perkin-Elmer (Norwalk, CT, USA) model 241 polarimeter equipped with a Haake (Karlsruhe, Germany) model D thermostat. Thin-layer chromatography was performed on Merck (Darmstadt, Germany) Kieselgel $60/F_{254}$ precoated plates using the following solvent systems: I, ($CHCl_3$–EtOH, 9 : 1); II, (Bu^nOH–AcOH–H_2O, 3 : 1 : 1); III, (toluene–EtOH, 7 : 1). The chromatograms were examined by UV fluorescence or developed by chlorine–starch–potassium iodide or ninhydrin chromatic reaction as appropriate. The four final products were also characterized by ESI-TOF (Perseptive Biosystem, Mariner, Foster City, CA) mass spectrometry.

Infrared Absorption

The solid-state infrared absorption spectra (KBr disk technique) were recorded with a Perkin-Elmer model 580 B spectrophotometer equipped with a Perkin-Elmer model 3600 IR data station. The solution spectra were obtained using a Perkin-Elmer model 1720 X FT–IR spectrophotometer, nitrogen-flushed and equipped with a sample-shuttle device, at 2 cm^{-1} nominal resolution, averaging 100 scans. Cells with path lengths of 0.1, 1.0, and 10 mm (with CaF_2 windows) were used. Spectrograde deuterochloroform (99.8% *d*) and deuterated DMSO (99.9% d_6) were purchased from Fluka (Buchs, Switzerland). Solvent (baseline) spectra were recorded under the same conditions.

NMR

The NMR spectra were recorded with a Bruker (Karlsruhe, Germany) model AM 400 spectrometer. Measurements were carried out in deuterated DMSO (99.96% d_6; Acros Organics, Geel, Belgium) with tetramethylsilane as the internal standard.

Cells and Virus

Vero cells were grown in DMEM supplemented with 10% fetal calf serum. HSV-1 carrying a LacZ gene driven by the CMV IE-1 promoter to express ß-galactosidase was propagated as previously described [14].

Inhibition of Virus Infectivity

Peptides were dissolved in DMEM without serum and used in a range of concentrations. All experiments were conducted in parallel with no peptide controls. To assess the effect of peptides on the inhibition of HSV infectivity, several different ways [15] of treating cell monolayers were followed:

(a) For the 'cell pre-exposure treatment', Vero cells were incubated with peptides (10, 50, 100, and 250 μM)

DOI: 10.1002/psc

for 30 min at 4 °C. Peptides were removed, and cells were washed with phosphate-buffered saline (PBS) before being infected with serial dilutions of HSV-1 and incubated for 45 min at 37 °C.

(b) For the 'co-exposure treatment', the cells were incubated with increasing concentrations of the peptides (10, 50, 100, and 250 μM) in the presence of the viral inoculum for 45 min at 37 °C.

(c) For the 'post-exposure treatment', Vero cell monolayers were challenged with HSV-1 for 45 min at 37 °C. Different concentrations of peptides (10, 50, 100, and 250 μM) were then added to the inoculum, followed by a further 30 min of incubation at 37 °C.

(d) For the 'virus pre-exposure treatment', HSV-1 (2×10^4 pfu) was incubated in the presence of different concentrations of peptides (10, 50, 100, and 250 μM) for 45 min at 37 °C, and then titrated on Vero cell monolayers.

For all treatments, nonpenetrated viruses were inactivated by a citrate buffer at pH 3.0 after 45 min incubation with cells at 37 °C. The cells were then incubated for 24 h at 37 °C in DMEM supplemented with CMC. Monolayers were fixed, stained with X-gal (5-bromo-4-chloro-3-indolyl-ß-D-galactopyranoside), and plaque numbers scored. Experiments were performed in triplicate and the percentage of inhibition was calculated with respect to no-peptide control experiments.

Cytotoxicity Evaluation

Peptide cytotoxicity was assessed by measuring the percentage of viable cells by the trypan blue exclusion and the LDH tests. After a 24-h period of incubation at 37 °C in a humidified 5% CO_2 atmosphere, cell monolayers were confluent, and the medium was removed from each well and replenished with 200 μl of peptide dilutions per well ranging from 5 to 500 μM prepared in DMEM. For the cell harvest, the medium was removed and the cells were washed twice with DMEM and trypsinized. For cell controls, 200 μl of DMEM without peptides were added.

For the trypan blue exclusion test, 0.5 ml of cell suspension were added to 50 μl of a 0.4% trypan blue solution. After 3 min, cells were counted in a hemocytometer chamber with a light microscope. The number of viable cells (those not taking up trypan blue) was divided by the total number of cells counted and multiplied by 100 to determine percent viable cells.

The LDH activity was carried out according to the manufacturer's instructions with a cytotoxicity detection kit (Boehringer, Mannheim, Germany). LDH is a stable cytoplasmic enzyme present in all cells and is rapidly released into the cell culture supernatant upon damage of the plasma membrane. The LDH activity was determined by a coupled enzymatic reaction whereby the tetrazolium salt was reduced to formazan. An increase in the number of dead or damaged cells resulted in an increase in LDH activity in the culture supernatant. The amounts of LDH showed that both treated and untreated cells were healthy. The LDH activity was measured spectrophotometrically by the change in absorbance at 340 nm at room temperature. The LDH released was calculated per cell; the LDH found in the medium of cells of treated groups was expressed as a percentage of that found in the control group for each experiment.

RESULTS AND DISCUSSION

Synthesis and Characterization of Peptides

For the large-scale production of the enantiomerically pure L-(αMe)Leu and L-(αMe)Val, we exploited an economically attractive and generally applicable chemoenzymatic synthesis developed by DSM Research (Geleen, The Netherlands) a few years ago [16,17]. It involves a combination of organic synthesis for the preparation of the α-amino acid amide followed by the use of a broadly specific α-amino acid amidase to achieve optical resolution.

The syntheses of the [L-Leu^6-OMe] synthetic precursor of halovir A and its [L-(αMe)Leu^3, L-Leu^6-OMe] and [L-(αMe)Val^4, L-Leu^6-OMe] analogues were performed in solution using the step-by-step strategy, beginning from the *C*-terminal H-L-Leu-OMe residue. C-activation was achieved by use of: (i) the EDC/HOBt method [18] for couplings involving protein amino acids; (ii) the EDC/HOAt method [19] for couplings involving the sterically demanding (αMe)Leu and (αMe)Val residues; and (iii) the 5(4*H*)-oxazolone method [20] for the introduction of the *N*-terminal Myr-Aib unit in the last step. The reaction yields were from modest (43%) to good (91%). The Hyp and Gln side chains were left unprotected. Removal of the Z N^{α}-protecting group was achieved by catalytic hydrogenation. Finally, the [L-Leu^6-OMe] analogue was submitted to chemical reduction (with $LiBH_4$ [21]) to afford halovir A. The serious solubility problems encountered in the syntheses of the *C*-terminal tri-, tetra-, and pentapeptides of [L-Leu^6-OMe] halovir A were almost completely overcome by operating in the more polar DMF (instead of CH_2Cl_2) as the reaction solvent.

The chemical and optical purities of all intermediates and final synthetic products, obtained in a chromatographically homogeneous state, were established by melting point determinations, TLC runs in three different solvent systems, and polarimetric and solid-state IR absorption measurements. Table 1 lists the physical and analytical properties for the newly synthesized peptides (i.e. those not described in Ref. 12). ^{1}H NMR spectra of all peptides and ESI-TOF mass spectra for the four final products (data not shown) confirmed the identity of the compounds synthesized.

DOI: 10.1002/psc

Table 1 Physical and analytical properties for the newly synthesized peptides

Peptide	Melting point (°C)	Recrystallization solvent[a]	$[\alpha]_D^{20}$ (°)[b]	TLC			IR (cm^{-1})[c]
				$R_{f\ I}$	$R_{f\ II}$	$R_{f\ III}$	
Z-L-Gln-L-Leu-OMe	154–155	CH_2Cl_2/LP	−30.9	0.45	0.75	0.15	3423, 3311, 1744, 1654, 1538
Z-L-Val-L-Gln-L-Leu-OMe	244–245	MeOH/DE	−13.0	0.45	0.80	0.15	3432, 3294, 1740, 1689, 1641, 1539
Z-L-Leu-L-Val-L-Gln-L-Leu-OMe	247–248	MeOH/DE	−10.5	0.45	0.85	0.15	3425, 3291, 1740, 1688, 1660, 1630, 1537
Z-L-Hyp-L-Leu-L-Val-L-Gln-L-Leu-OMe	262–263	MeOH/DE	−47.5	0.15	0.70	0.05	3439, 3276, 1742, 1704, 1659, 1635, 1545
Z-L-(αMe)Leu-L-Val-L-Gln-L-Leu-OMe	177–178	EtOAc/LP	−42.3[d]	0.75	0.90	0.25	3415, 3304, 1731, 1662, 1645, 1535
Z-L-Hyp-L-(αMe)Leu-L-Val-L-Gln-L-Leu-OMe	114–115	EtOAc/LP	−52.6[d]	0.25	0.85	0.15	3311, 1741, 1662, 1641, 1541
[L-(αMe)Leu^3, L-Leu^6-OMe] halovir A	158–159	CH_2Cl_2/LP	−9.5[d]	0.10	0.80	0.10	3415, 3267, 1741, 1644, 1549
Z-L-(αMe)Val-L-Gln-L-Leu-OMe	161–162	CH_2Cl_2/DE	−35.4[d]	0.45	0.95	0.15	3415, 3303, 1745, 1706, 1653, 1532
Z-L-Leu-L-(αMe)Val-L-Gln-L-Leu-OMe	73–74	CH_2Cl_2/DE	−36.9[d]	0.45	0.95	0.15	3313, 1739, 1661, 1525
Z-L-Hyp-L-Leu-L-(αMe)Val-L-Gln-L-Leu-OMe	86–88	CH_2Cl_2/DE	−78.1[d]	0.15	0.95	0.05	3320, 1741, 1664, 1528
[L-(αMe)Val^4, L-Leu^6-OMe] halovir A	161–162	CH_3CN	−9.8[d]	0.05	0.95	0.05	3423, 3313, 1748, 1642, 1541

[a] LP, light petroleum; MeOH, methanol; DE, diethyl ether; EtOAc, ethyl acetate.
[b] $c = 0.1$, DMF.
[c] The IR absorption spectra were obtained in KBr pellets. Only significant bands in the 3500–3200 and 1800–1500 regions are listed.
[d] $c = 0.5$, MeOH.

DOI: 10.1002/psc

Conformational Analysis

The FT-IR absorption spectra in $CDCl_3$ solution clearly indicate that the fully protected, *C*-terminal, tri-, tetra-, and pentapeptides of [L-Leu^6-OMe] halovir A, as also suggested by their poor solubility properties, tend to effectively self-associate into β-sheet structures. This conclusion is based on the occurrence of strong bands in the amide N–H stretching region at 3286–3268 cm^{-1} and in the C=O stretching region at about 1630 cm^{-1} [22,23] (Figures 1(A) and 2, respectively). The β-sheet structure is sensitive to the addition of DMSO, which is capable of interacting with the peptide NH groups. For the pentapeptide, 40% DMSO (v/v) is enough to disrupt almost completely the self-associated species (Figure 2). A similar dissociative effect on the intermolecular β-sheet structure induced by a so-called '*chemical chaperone*' (e.g. DMSO) was recently reported for a protected pentapeptide related to the β-amyloid sequence 17–21 [24]. Incorporation of either L-(αMe)Leu or L-(αMe)Val in an internal position of the sequence (for the latter analogue see Figure 1(B)) prevents the strong self-association phenomenon by inducing the onset of intramolecularly H-bonded NH groups to a significant extent (helix formation), the corresponding band of which is seen near 3335 cm^{-1} [22]. Disruption of the intermolecular β-sheet structure in model and bioactive peptides by insertion of a C^{α}-tetrasubstituted α-amino acid and its assessment by the FT-IR absorption technique are well established [24,25]. Interestingly, a partial self-aggregation is exhibited by all three helical hexapeptides (for two of them, see Figure 1(A) and (B)) by virtue of their lipophilic, myristoyl chain at the *N*-terminus despite the presence of one (or two) C^{α}-tetrasubstituted α-amino acid(s) in their sequences.

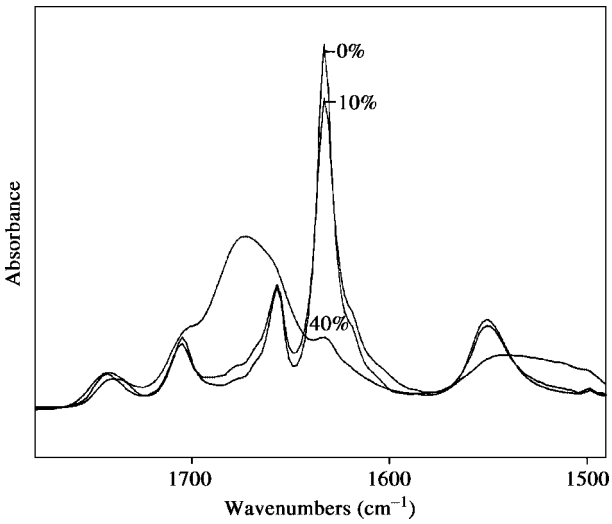

Figure 2 FT-IR absorption spectra in the C=O stretching region of *Z*-L-Hyp-L-Leu-L-Val-L-Gln-L-Leu-OMe in $CDCl_3$ solutions containing the indicated percentages of DMSO. Peptides concentration: 1mM.

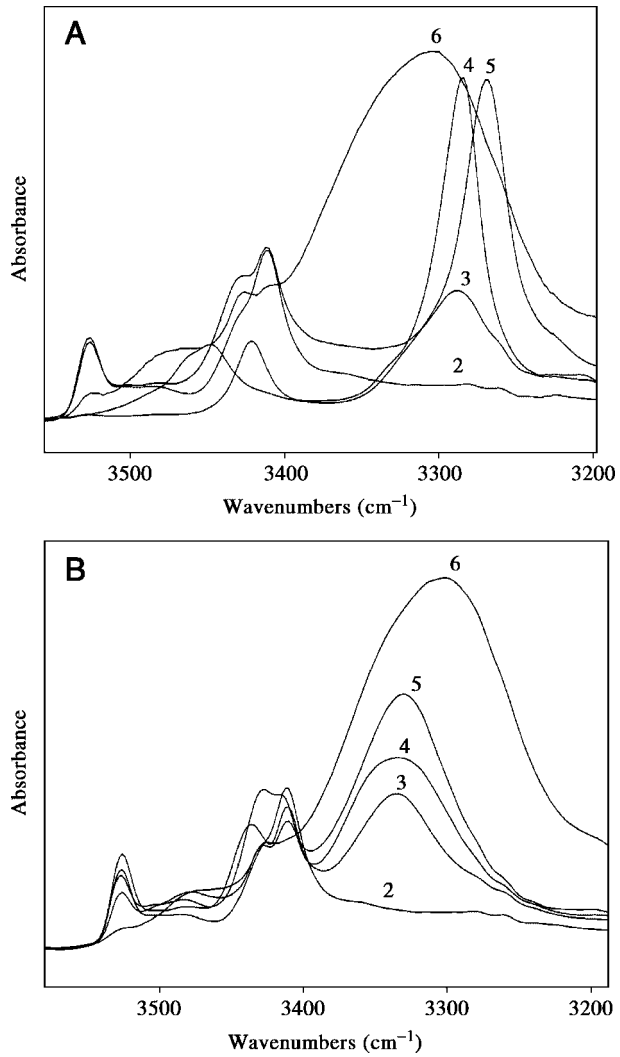

Figure 1 (A) FT-IR absorption spectra in the N–H stretching region of [L-Leu^6-OMe] halovir A (6) and its shorter *C*-terminal sequences (5–2) in $CDCl_3$ solution. Peptide concentration: 1mM. (B) Same series of spectra for [L-(αMe)Val^4, L-Leu^6-OMe] halovir A.

More detailed conformational information was extracted from an NMR investigation of the three hexapeptides in DMSO-d_6 solution. All NH proton resonances were assigned by means of ROESY and TOCSY experiments (mixing times, 200 ms and 70 ms, respectively). The chemical shifts of the two C^{α}-methylated hexapeptides are quite close to the corresponding ones characterizing the spectrum of the parent [L-Leu^6-OMe] halovir A. They also compare well with those of halovir A itself. Three strong, sequential $d_{NN}(i, i+1)$ cross peaks were observed in the ROESY spectrum of [L-(αMe)Val^4, L-Leu^6-OMe] halovir A between the Leu^3, (αMe)Val^4, Gln^5, and Leu^6 residues (Figure 3). Such inter-residue correlations are a distinctive feature of peptides largely folded in a well-developed helical conformation [26]. The known propensity of an Aib-Hyp (or Pro) sequence to reside in the *trans* peptide conformation [27,28] was confirmed by the observation of two

DOI: 10.1002/psc

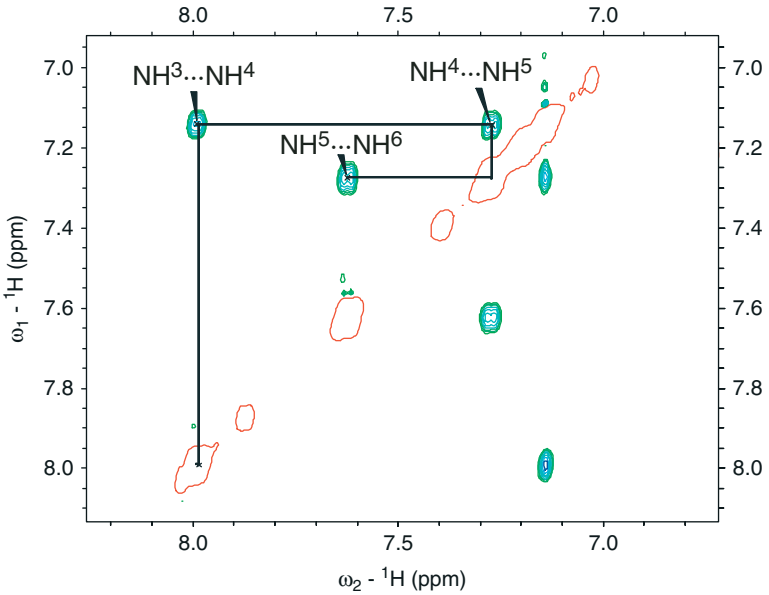

Figure 3 Partial ROESY spectrum of [L-(αMe)Val^4, L-Leu^6-OMe] halovir A in DMSO-d_6 solution showing intense $d_{NN}(i, i+1)$ cross peaks, indicative of a helical structure.

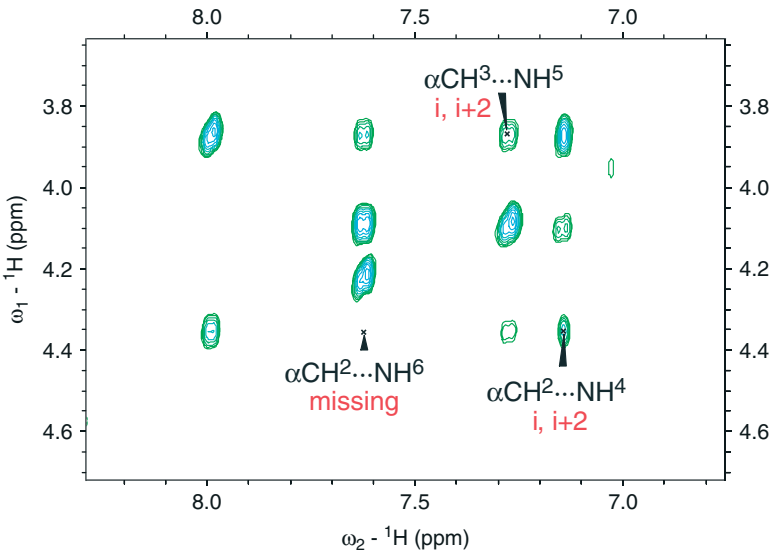

Figure 4 Partial ROESY spectrum of [L-(αMe)Val^4, L-Leu^6-OMe] halovir A in DMSO-d_6 solution showing intense $d_{\alpha N}(i, i+2)$ cross peaks, typical of the 3_{10}-helix. The area in the spectrum, where the only potentially observable, but undetected, $d_{\alpha N}(i, i+4)$ cross peak, typical of the α-helical structure, was expected, is also indicated.

Aib^{1}NH···Hyp^{2}δCH$_2$ cross peaks (that with the lower field δCH is stronger) and one Leu^{3}NH···Hyp^{2}δCH (at higher field) cross peak (not shown) [26]. Similar 2D NMR spectra in the NH···NH region were obtained for the other two hexamers (not shown). All correlations match well with those already reported for halovir A [9]. In the ROESY spectrum of [L-(αMe)Val^4, L-Leu^6-OMe] halovir A (Figure 4) two $d_{\alpha N}(i, i+2)$ cross peaks indicative of the 3_{10}-helical structure [26] are seen, between Hyp^{2}αCH and (αMe)Val^4 NH, and between Leu^{3}αCH and Gln^5 NH. The corresponding ROESY spectrum of [L-(αMe)Leu^3, L-Leu^6-OMe] halovir A (not shown) is also characterized by two $d_{\alpha N}(i, i+2)$ cross peaks, between Hyp^{2}αCH and Val^4 NH, and between Val^{4}αCH and Leu^6 NH. Conversely, only one (out of the three possible) $d_{\alpha N}(i, i+2)$ cross peak, Hyp^{2}αCH···Val^4 NH, was clearly measured for halovir A [9] and its [L-Leu^6-OMe] analogue (not shown). Interestingly, in any of the ROESY spectra of halovir A [9] and its three analogues (for one of them, see Figure 4), the only possible $d_{\alpha N}(i, i+4)$ cross peak, Hyp^{2}αCH···Leu^6(Lol) NH, typical of an α-helical structure [26], is observed.

DOI: 10.1002/psc

Taken together, these FT-IR absorption and NMR findings strongly support the view that all three halovir A hexapeptide analogues are characterized by a strong tendency to fold into a 3_{10}-helical structure. This propensity seems to be slightly more pronounced for the [L-(αMe)Leu^3, L-Leu^6-OMe] and [L-(αMe)Val^4, L-Leu^6-OMe] analogues.

Antiviral and Cytotoxic Activities

The halovirs possess potent *in vitro* activity against HSV-1 [9,12]. Several experiments were performed to provide insight into possible mechanisms involved in the antiviral activities of halovir A (**peptide 1**) and its three analogues, [L-Leu^6-OMe] (**peptide 2**), [L-(αMe)Leu^3, L-Leu^6-OMe] (**peptide 3**), and [L-(αMe)Val^4, L-Leu^6-OMe] (**peptide 4**).

Some of the peptides tested showed a dose-dependent inhibition of HSV entry either if present on the monolayers together with the virus inoculum for the 45 min (Figure 5(A)) or when the virus was pre-incubated with peptides for 1 h at 37°C before addition to the cells (Figure 5(B)). As shown in Figure 5(A), while **peptides 1** and **3** were inactive in reducing HSV-1 infectivity, **peptide 2** progressively reduced infection as the concentration of the compound increased, reaching an inhibition value of about 50%. The most active compound was **peptide 4**. With **peptide 4** at concentration of 50 μM, the reduction of infectivity was already about 50%, while it reached a value of about 90% at a concentration of 250 μM. The antiviral efficacy of peptides is greater when they are incubated with HSV-1 prior to exposure to Vero cell monolayers. Figure 5(B) shows that the **peptides 2** and **4** inactivate the virus in a concentration-dependent manner demonstrating a virucidal mechanism of action.

Further experiments were carried out to investigate the step in the entry process that was inhibited by the peptides. We chose a peptide concentration (250 μM) that gave a significant antiviral activity in the previous experiment (co-exposure treatment), and compared the effect of two more methods of exposure of the cells to peptide (Figure 6). The data obtained showed that the exposure of the cell to the peptide concomitantly with the virus represents the stage of optimal infectivity reduction. This finding could be explained by a possible interaction of the compound

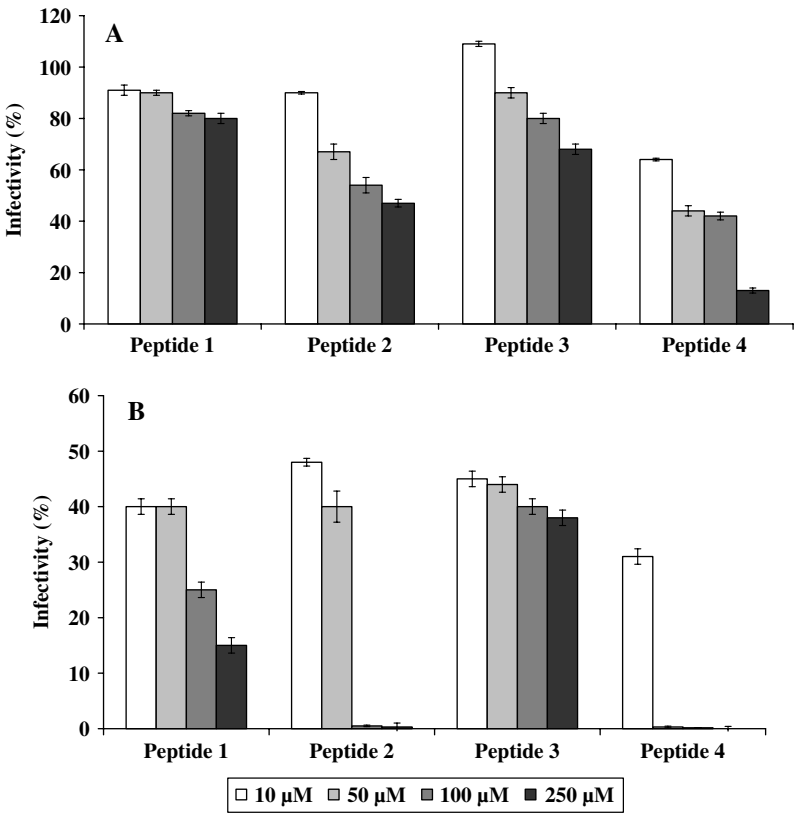

Figure 5 Dose-dependent inactivation of HSV-1 by peptides. (A) (co-exposure): Vero cells were incubated with increasing concentrations of peptides (10, 50, 100, and 250 μM) in the presence of the viral inoculum for 45 min at 37°C; (B) (virus pre-exposure): the virus was pre-incubated with peptides for 1 h at 37°C before addition to the cells. Nonpenetrated virus was inactivated and cells incubated for 24 h at 37°C in DMEM supplemented with CMC. Plaque numbers were scored and the percentage of inhibition was calculated with respect to no-peptide control experiments. Data are reported in triplicate and error bars represent standard deviations.

DOI: 10.1002/psc

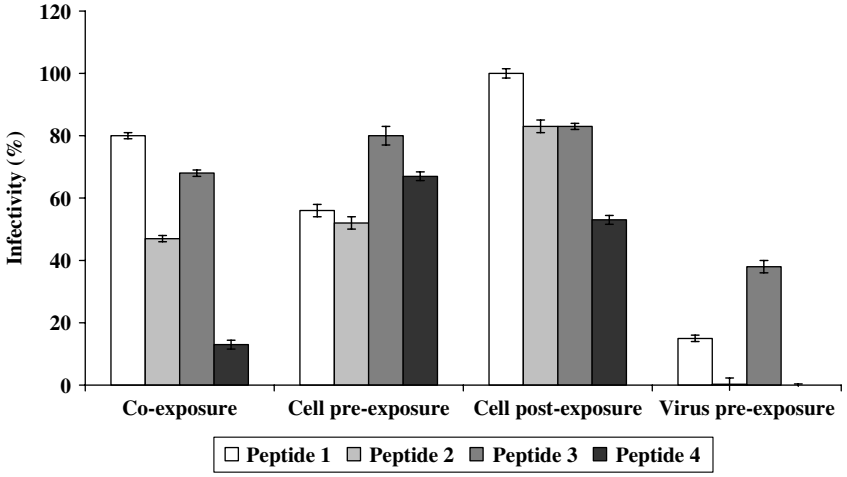

Figure 6 Analysis of virus infectivity inhibition by halovir A (**peptide 1**) and its three analogues (**peptides 2–4**). Vero cells were exposed to peptides (250 μM concentration) either during attachment and entry (co-exposure), or prior to infection (cell pre-exposure), or after virus penetration (post-exposure), or alternatively, the virus was pre-incubated with peptides for 1 h at 37 °C before addition to the cells (virus pre-exposure). For all treatments, nonpenetrated viruses were inactivated by a low-pH citrate buffer after the 45-min incubation with cells at 37 °C. The cells were then incubated for 24 h at 37 °C in DMEM supplemented with CMC. Experiments were performed in triplicate and the percentage of inhibition was calculated with respect to no-peptide control experiments. Error bars represent standard deviations.

with either the virus or the cells at the specific stage of binding/penetration of the virus into the cells. When performing experiments in which cells were treated with the peptide prior to virus infection, the effect of the peptide was markedly reduced. Therefore, we assume that the inhibitory effect is not merely due to cell membrane conditioning. Surprisingly, **peptide 1** was more active in this experiment than in the previous one. Finally, we tested the peptides once the cells were already infected; the main conclusion that can be drawn is that only **peptide 4** has an activity, even though less pronounced compared to the co-exposure treatment, in a post-entry stage.

At present, we are unable to unambiguously delineate the mechanism of action of **peptide 4** following viral penetration, but either it may penetrate into the cells and interfere with one of the several post-entry events (uncoating, transcription, translation, genome replication, assembly, envelopment, exit) of the replication cycle or it may remain on the cell surface and stop the viral spread. The second possibility seems to be the most probable one considering the relatively high concentration needed to observe an infectivity reduction.

To rule out cytotoxic effects on Vero cells, monolayers were exposed to different concentrations (5, 10, 50, 100, 250, and 500 μM) of each peptide for 24 h, and cell viability was checked by an LDH assay and a trypan blue exclusion test. Using either method, no statistical difference was observed between the viability of untreated cells and that of cells exposed to the peptides (Figure 7). A minimal cytotoxic effect of the peptides was seen at concentrations much higher than those used in the antiviral assays (data not shown).

CONCLUSIONS

In this work we have set up a synthetic route in solution that allows one to produce chemically and optically pure halovir A analogues containing helicogenic C^{α}-tetrasubstituted α-amino acid in satisfactory yields. Our conformational analysis using FT-IR absorption and NMR has established that incorporation of a second C^{α}-tetrasubstituted α-amino acid [either L-(αMe)Leu at position 3 or L-(αMe)Val at position 4] does increase, but only slightly, the extent of right-handed 3_{10}-helical conformation characterizing halovir A [9].

Natural halovirs and other linear peptides have been reported to inhibit HSV-1 infectivity [9,12,29–31]. Our results confirm and expand these data in the sense that **peptide 2** and particularly **peptide 4** are potent inhibitors of HSV-1 infectivity. Quite reasonably, this bioactivity is related to the ternary helicity and the resulting amphiphilicity of the halovir peptides, as proposed by Rowley *et al.* [9].

Our hypothesis is that the halovir analogue showing the strongest activity (**peptide 4**) may act by a mechanism based on membrane destabilization. Interestingly, the viral envelope is known to be more sensitive to membrane disruption than the host cell plasma membrane. Virus particle inactivation would represent an ideal method for rendering HSV noninfectious, thereby limiting its diffusion especially when considering the genital route. Our results tend to support the view that the antiviral activity of halovirs might be due to an unspecific interaction with the viral envelope and that the membrane curvature of the viral envelope would be a key factor for their potential antiviral effect. Interestingly, our experiments demonstrate a clear antiviral

DOI: 10.1002/psc

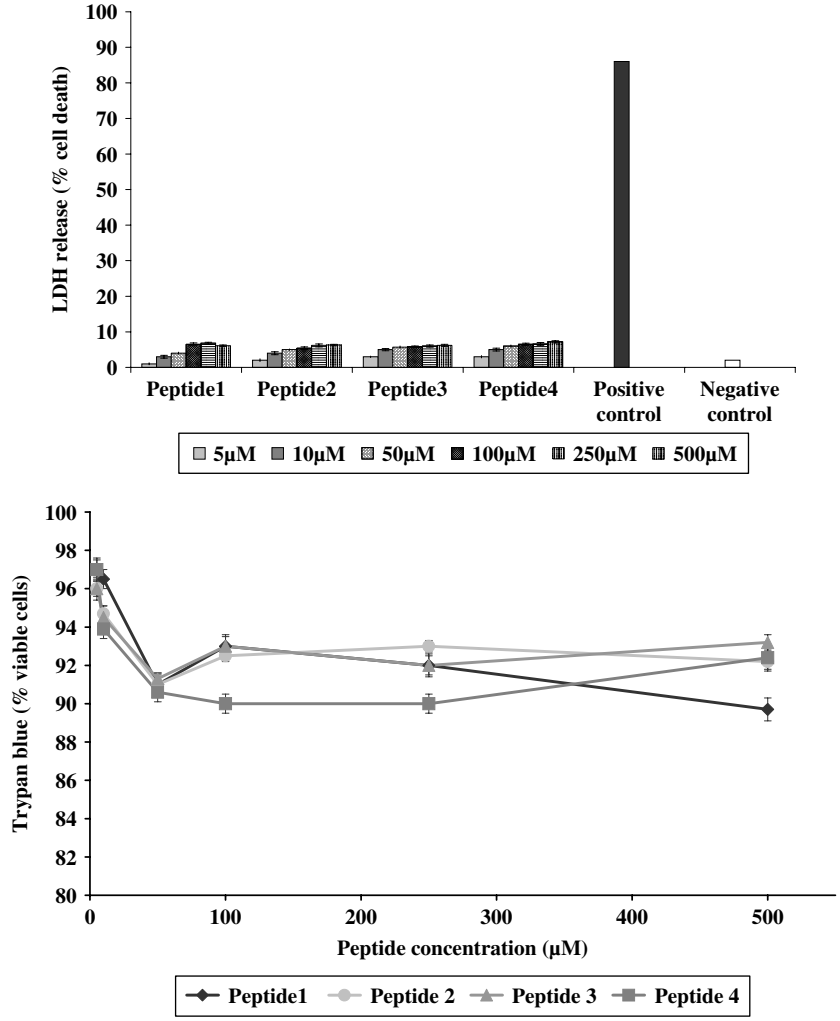

Figure 7 Effect of halovir A (**peptide 1**) and its three analogues (**peptides 2–4**) on cell viability. Peptide cytotoxicity was assessed by measuring the percentage of viable cells by the LDH and the trypan blue exclusion tests. The data are the average from three different experiments, and the error bars indicate the standard errors of the means.

activity of halovirs against HSV-1 at concentrations nontoxic to cultured Vero cells. In any case, additional studies are needed to assess the antiviral activity of our compounds against other enveloped viruses.

In summary, these promising findings encourage us to further investigate this type of conformationally constrained peptide analogues of halovir A as antiviral candidates of pharmaceutical interest.

REFERENCES

1. Benedetti E, Bavoso A, Di Blasio B, Pavone V, Pedone C, Toniolo C, Bonora GM. Peptaibol antibiotics: a study on the helical structure of the 2–9 sequence of emerimicins III and IV. *Proc. Natl. Acad. Sci. U.S.A.* 1982; **79**: 7951–7954.
2. Brückner H, Graf H. Paracelsin, a peptide antibiotic containing α-aminoisobutyric acid, isolated from *Trichoderma reesei* Simmons. *Experientia* 1983; **39**: 528–530.
3. Sansom MSP. The biophysics of peptide models of ion channels. *Prog. Biophys. Mol. Biol.* 1991; **55**: 139–235.
4. Rebuffat S, Goulard C, Bodo B, Roquebert M-F. The peptaibol antibiotics from *Trichoderma* soil fungi: structural diversity and membrane properties. *Recent Res. Devel. Org. Biorg. Chem.* 1999; **3**: 65–91.
5. Toniolo C, Crisma M, Formaggio F, Peggion C, Epand RF, Epand RM. Lipopeptaibols, a novel family of membrane active, antimicrobial peptides. *Cell. Mol. Life Sci.* 2001; **58**: 1179–1188.
6. Whitmore L, Chugh JK, Snook CF, Wallace BA. The peptaibol database: a sequence and structure resource. *J. Pept. Sci.* 2003; **9**: 663–665.
7. Karle IL, Balaram P. Structural characteristics of α-helical peptide molecules containing Aib residues. *Biochemistry* 1990; **29**: 6747–6756.
8. Toniolo C, Crisma M, Formaggio F, Peggion C. Control of peptide conformation by the Thorpe-Ingold effect (C^{α}-tetrasubstitution). *Biopolymers (Pept. Sci.)* 2001; **60**: 396–419.
9. Rowley DC, Kelly S, Kauffman CA, Jensen PR, Fenical W. Halovirs A-E, new antiviral agents from a marine-derived fungus of the genus *Scytalidium*. *Bioorg. Med. Chem.* 2003; **11**: 4263–4274.
10. Stanberry LR, Jorgensen DM, Nahmias AJ. Herpes simplex viruses 1 and 2. In *Viral Infections of Humans: Epidemiology and Control*, Evans AS, Kaslow RA (eds), 4th edn. Plenum Medical Book Company: New York, 1997; 419–454.

DOI: 10.1002/psc

11. Toniolo C, Benedetti E. The polypeptide 3_{10}-helix. *Trends Biochem. Sci.* 1991; **16**: 350–353.
12. Rowley DC, Kelly S, Jensen P, Fenical W. Synthesis and structure-activity relationships of the halovirs, antiviral natural products from a marine-derived fungus. *Bioorg. Med. Chem.* 2004; **12**: 4929–4936.
13. Toniolo C, Crisma M, Formaggio F, Valle G, Cavicchioni G, Précigoux G, Aubry A, Kamphuis J. Structures of peptides from α-amino acids methylated at the α-carbon. *Biopolymers* 1993; **33**: 1061–1072.
14. Forrester A, Farrell H, Wilkinson G, Kaye J, Davis-Poynter N, Minson T. Construction and properties of a mutant of herpes simplex virus type 1 with glycoprotein H coding sequences deleted. *J. Virol.* 1992; **66**: 341–348.
15. Galdiero S, Vitiello M, D'Isanto M, Falanga A, Collins C, Raieta K, Pedone C, Browne H, Galdiero M. Analysis of synthetic peptides from heptad-repeat domains of herpes simplex virus type 1 glycoproteins H and B. *J. Gen. Virol.* 2006; **87**: 1085–1097.
16. Kruizinga WH, Bolster J, Kellogg RM, Kamphuis J, Boesten WHJ, Meijer EM, Schoemaker HE. Synthesis of optically pure α-alkylated α-amino acids and a single-step method for enantiomeric excess determination. *J. Org. Chem.* 1988; **53**: 1826–1827.
17. Schoemaker HE, Boesten WHJ, Kaptein B, Hermes HFM, Sonke T, Broxterman QB, van den Tweel WHJ, Kamphuis J. Chemo-enzymatic synthesis of amino acids and derivatives. *Pure Appl. Chem.* 1992; **64**: 1171–1175.
18. König W, Geiger R. Eine neue Methode zur Synthese von Peptiden: Aktivierung der Carboxylgruppe mit Dicyclohexylcarbodiimid unter Zusatz von 1-Hydroxy-benzotriazolen. *Chem. Ber.* 1970; **103**: 788–798.
19. Carpino LA. 1-Hydroxy-7-azabenzotriazole. An efficient peptide coupling additive. *J. Am. Chem. Soc.* 1993; **115**: 4397–4398.
20. Jones DS, Kenner GW, Preston J, Sheppard RC. Peptides. Part XVII. Synthesis of peptides and polymers of some sterically hindered amino acids via oxazolone intermediates. *J. Chem. Soc.* 1965; 6227–6239.
21. Brown HC, Narasimhan S. New powerful catalysts for the reduction of esters by lithium borohydride. *J. Org. Chem.* 1982; **47**: 1604–1606.
22. Palumbo M, Da Rin S, Bonora GM, Toniolo C. Linear oligopeptides. 29. Infrared conformational analysis of homo-oligopeptides in the solid state and in solution. *Makromol. Chem.* 1976; **177**: 1477–1492.
23. Toniolo C, Bonora GM, Marchiori F, Borin G. An infrared absorption method to titrate quantitatively the extent of self-association in peptides. *J. Am. Chem. Soc.* 1984; **106**: 1455–1457.
24. Formaggio F, Bettio A, Moretto V, Crisma M, Toniolo C, Broxterman QB. Distruption of the β-sheet structure of a protected pentapeptide, related to the β-amyloid sequence 17–21, induced by a single, helicogenic, C^{α}-tetrasubstituted α-amino acid. *J. Pept. Sci.* 2003; **9**: 461–466.
25. Moretto V, Crisma M, Bonora GM, Toniolo C, Balaram H, Balaram P. Comparison of the effect of five guest residues on the β-sheet conformation of host $(L\text{-Val})_n$ homo-oligopeptides. *Macromolecules* 1989; **22**: 2939–2944.
26. Wüthrich K. *NMR of Proteins and Nucleic Acids*. Wiley: New York, 1986; 192–196.
27. Venkatachalapathi YV, Nair CMK, Vijayan M, Balaram P. X-Pro peptides: solution and solid-state conformation of benzyloxycarbonyl-$(Aib\text{-}Pro)_2$-methyl ester, a type-I β-turn. *Biopolymers* 1981; **20**: 1123–1136.
28. Di Blasio B, Pavone V, Saviano M, Lombardi A, Nastri F, Pedone C, Benedetti E, Crisma M, Anzolin M, Toniolo C. Structural characterization of the β-bend ribbon spiral: crystallographic analysis of two long $(L\text{-Pro-Aib})_n$ sequential peptides. *J. Am. Chem. Soc.* 1992; **114**: 6273–6278.
29. Baghian A, Jaynes J, Enright F, Kousoulas KG. An amphipathic α-helical synthetic peptide analogue of melittin inhibits herpes simplex virus-1 (HSV-1)-induced cell fusion and virus spread. *Peptides* 1997; **18**: 177–183.
30. Bultmann H, Busse JS, Brandt CR. Modified FGF4 signal peptide inhibits entry of herpes simplex virus type 1. *J. Virol.* 2001; **75**: 2634–2645.
31. Jenssen H, Andersen JH, Mantzilas D, Gutteberg TJ. A wide range of medium-sized, highly cationic, α-helical peptides show antiviral activity against herpes simplex virus. *Antiviral Res.* 2004; **64**: 119–126.